

**Effect of external stress on ferroelectricity in epitaxial thin films**A. Yu. Emelyanov,<sup>1,2</sup> N. A. Pertsev,<sup>1,\*</sup> and A. L. Kholkin<sup>2</sup><sup>1</sup>*A. F. Ioffe Physico-Technical Institute, Russian Academy of Sciences, 194021 St. Petersburg, Russia*<sup>2</sup>*Department of Ceramic and Glass Engineering, CICECO, University of Aveiro, 3810-193 Aveiro, Portugal*

(Received 10 July 2002; published 20 December 2002)

A nonlinear thermodynamic theory is used to describe the influence of an external mechanical loading on the ferroelectric, dielectric, and piezoelectric properties of epitaxial thin films grown on dissimilar cubic substrates. The calculations are performed for single-domain perovskite films in the approximation of a homogeneous loading of the film upper surface. The “misfit strain-stress” and “stress-temperature” phase diagrams are developed for epitaxial PbTiO<sub>3</sub> and BaTiO<sub>3</sub> films. It is shown that the loading may lead to drastic changes of the film polarization state. The most remarkable theoretical prediction is the stress-induced ferroelectric to paraelectric phase transition, which may take place at room temperature in films grown on “compressive” substrates that provide large negative misfit strains in the epitaxial system. The small-signal dielectric and piezoelectric constants of single-domain PbTiO<sub>3</sub> and BaTiO<sub>3</sub> films are also calculated and found to be very sensitive to the external stress under certain misfit strain-temperature conditions. The theory thus predicts that the mechanical loading of ferroelectric films can be employed for the fine tuning of their physical properties. The results of calculations may be also useful for the interpretation of experimental data obtained via scanning force microscopy and the indentation of ferroelectric films.

DOI: 10.1103/PhysRevB.66.214108

PACS number(s): 77.55.+f, 77.80.-e, 77.22.Ch

**I. INTRODUCTION**

It is well known that ferroelectric, dielectric, and piezoelectric properties of thin films may differ markedly from those of bulk ferroelectrics. These differences are partly due to the straining and two-dimensional clamping of the film by a dissimilar thick substrate. To quantify this mechanical substrate effect, “misfit strain-temperature” phase diagrams were developed for epitaxial ferroelectric films using a nonlinear thermodynamic theory.<sup>1-7</sup> In all performed theoretical studies, it was assumed that there are no external mechanical forces acting on the upper surface of the film. This situation is indeed typical of the polarization and dielectric measurements, where the film is practically free to deform in the out-of-plane directions. However, experimental studies of the direct piezoelectric effect require an external loading of the free surface.<sup>8</sup> The microindentation of ferroelectric thin films, which represents a useful technique to study their local depolarization properties,<sup>9</sup> is accompanied by the high mechanical stresses appearing under the metallic indenter.

Moreover, the mechanical loading of the film surface is a characteristic feature of the scanning force microscopy (SFM) operated in the piezoelectric contact mode.<sup>10</sup> The SFM piezoresponse imaging method, which is widely used by many researchers for the characterization of ferroelectric films on the nanometer scale,<sup>11</sup> involves the application of an electric field between the conductive SFM tip and the bottom electrode. The electrostatic attraction (Maxwell force) between this electrode and the tip/cantilever system produces a force pressing the tip to the film surface.<sup>10</sup> An additional mechanical force may be applied to the tip intentionally in order to create high local stresses in the measurement area.<sup>10,12</sup> It was found that the effective piezoelectric coefficient of lead zirconate titanate films appreciably decreases with the increase of the force acting on the tip.<sup>12</sup> Based on SFM studies of BaTiO<sub>3</sub> thin films in the piezoresponse

mode, the authors of Ref. 10 proposed that the simultaneous application of electric field and compressive stress may induce a ferroelastoelectric switching in the film, resulting in the orientation of spontaneous polarization *antiparallel* to the applied electric field.

The correct interpretation of effects observed via SFM, microindentation, and other stress-inducing techniques requires the development of a *nonlinear* thermodynamic theory of ferroelectric thin films subjected to mechanical loading. Indeed, the order parameters (polarization components) in ferroelectric films may dramatically change with variations of lattice strains.<sup>1-7</sup> The account of strain inhomogeneity in a loaded film, however, will make the nonlinear theory extremely complicated, as can be deduced from the solutions obtained for linear elastic and piezoelectric solids subjected to spherical indentation.<sup>13-16</sup> Therefore, it is worthwhile to study first the case of uniform loading of an epitaxial film.

In this paper, a nonlinear thermodynamic theory is developed for uniformly loaded single-domain ferroelectric films, where the formation of elastic domains (twins) is assumed to be suppressed, e.g., due to kinetic reasons. It is shown that the external loading may lead to drastic changes of the polarization state of the film. Though our solution cannot be directly applied to the interpretation of the SFM data, it provides better understanding of the ferroelectric behavior of loaded epitaxial films and represents a necessary first step in the development of the general nonlinear theory.

**II. NONLINEAR THERMODYNAMIC THEORY**

Consider a single-crystalline perovskite thin film epitaxially grown in a paraelectric state on a dissimilar cubic substrate. Since changes of the in-plane lattice strains  $S_1$ ,  $S_2$ , and  $S_6$  in the overlayer during cooling or mechanical loading of the heterostructure are controlled by a much thicker substrate, the standard elastic Gibbs function  $G$  cannot be used

to determine the equilibrium thermodynamic states of an epitaxial film.<sup>1</sup> (We use the Voigt matrix notation and the rectangular reference frame with the  $x_3$  axis orthogonal to the substrate surface.) When the film/substrate system is subjected to external mechanical forces, the Helmholtz free-energy function  $F$  is not appropriate for the thermodynamic description of the film as well. We may assume, however, that the epitaxial single-domain film has three fixed lattice strains ( $S_1$ ,  $S_2$ , and  $S_6$ ) and three constant internal stresses ( $\sigma_3$ ,  $\sigma_4$ , and  $\sigma_5$ ). For these mixed mechanical conditions, a modified thermodynamic potential  $\tilde{G}$  introduced in Ref. 1 must be used in the theoretical calculations.

The potential  $\tilde{G}$  of a ferroelectric film may be found in an explicit form using the relation  $\tilde{G} = G + S_1\sigma_1 + S_2\sigma_2 + S_6\sigma_6$  and specifying the Gibbs function  $G$ . For perovskite ferroelectrics like  $\text{PbTiO}_3$  and  $\text{BaTiO}_3$ , this function may be approximated by a six-degree polynomial in polarization components  $P_i$  ( $i=1,2,3$ ).<sup>17,18</sup> In the crystallographic reference frame, which can be directly employed in the case of (001)-oriented films considered in this paper, the function  $G$  has a well-known standard form.<sup>1,4,17,18</sup> The resulting expression for the modified potential shows that  $\tilde{G}$  is a function of the polarization components  $P_i$ , stresses  $\sigma_n$  ( $n=1,2,3,\dots,6$ ), and strains  $S_1$ ,  $S_2$ , and  $S_6$ . Assuming that the film is grown on a cubic substrate with the surface parallel to the (001) crystallographic plane, we have  $S_1=S_2=S_m$  and  $S_6=0$ , where  $S_m=(b^*-a_0)/a_0$  is the misfit strain in the epitaxial system ( $b^*$  is the substrate effective lattice parameter,<sup>19</sup> and  $a_0$  is the equivalent cubic cell constant of the free standing film). The stress  $\sigma_3$  in a single-domain film is governed by the applied load and will be regarded as a given external parameter throughout this paper, whereas the shear stresses  $\sigma_4$  and  $\sigma_5$  will be neglected ( $\sigma_4=\sigma_5=0$ ). The remaining components  $\sigma_1$ ,  $\sigma_2$ , and  $\sigma_6$  of the stress tensor depend on the misfit strain  $S_m$ , external stress  $\sigma_3$ , and on the polarizations  $P_i$ . Explicit expressions for these stresses can be easily derived using the stress-strain relationships<sup>18</sup>  $S_n = -\partial G/\partial \sigma_n$  together with the strain conditions  $S_1=S_2=S_m$  and  $S_6=0$ . The substitution of these expressions into the basic formula for the modified thermodynamic potential transforms  $\tilde{G}$  into a function of three independent variables:  $P_1$ ,  $P_2$ , and  $P_3$ . After some algebraic rearrangement,  $\tilde{G}$  can be cast into the form

$$\begin{aligned} \tilde{G} = & \frac{(S_m - s_{12}\sigma_3)^2}{s_{11} + s_{12}} - \frac{1}{2}s_{11}\sigma_3^2 + a_1^*(P_1^2 + P_2^2) + a_3^*P_3^2 \\ & + a_{11}^*(P_1^4 + P_2^4) + a_{12}^*P_1^2P_2^2 + a_{13}^*(P_1^2 + P_2^2)P_3^2 + a_{33}^*P_3^4 \\ & + a_{111}(P_1^6 + P_2^6 + P_3^6) + a_{112}[P_1^4(P_2^2 + P_3^2) + P_2^4(P_1^2 + P_3^2) \\ & + P_3^4(P_1^2 + P_2^2)] + a_{123}P_1^2P_2^2P_3^2, \end{aligned} \quad (1)$$

where

$$a_1^* = a_1 - \frac{Q_{11} + Q_{12}}{s_{11} + s_{12}} S_m + \frac{Q_{11}s_{12} - Q_{12}s_{11}}{s_{11} + s_{12}} \sigma_3, \quad (2)$$

$$a_3^* = a_1 - \frac{2Q_{12}}{s_{11} + s_{12}} S_m - \left( Q_{11} - \frac{2Q_{12}s_{12}}{s_{11} + s_{12}} \right) \sigma_3, \quad (3)$$

$$a_{11}^* = a_{11} + \frac{1}{2} \frac{1}{s_{11}^2 - s_{12}^2} [(Q_{11}^2 + Q_{12}^2)s_{11} - 2Q_{11}Q_{12}s_{12}], \quad (4)$$

$$a_{33}^* = a_{11} + \frac{Q_{12}^2}{s_{11} + s_{12}}, \quad (5)$$

$$a_{12}^* = a_{12} - \frac{1}{s_{11}^2 - s_{12}^2} [(Q_{11}^2 + Q_{12}^2)s_{12} - 2Q_{11}Q_{12}s_{11}] + \frac{Q_{44}^2}{2s_{44}}, \quad (6)$$

$$a_{13}^* = a_{12} + \frac{Q_{12}(Q_{11} + Q_{12})}{s_{11} + s_{12}}. \quad (7)$$

In Eqs. (1)–(7),  $a_1$ ,  $a_{ij}$ , and  $a_{ijk}$  are the dielectric stiffness and higher-order stiffness coefficients at constant stress,<sup>17,18</sup>  $s_{ln}$  are the elastic compliances at constant polarization, and  $Q_{ln}$  are the electrostrictive constants of the paraelectric phase. The dielectric stiffness  $a_1$  should be given a linear temperature dependence  $a_1 = (T - \theta)/2\varepsilon_0 C$  based on the Curie-Weiss law ( $\theta$  and  $C$  are the Curie-Weiss temperature and constant, and  $\varepsilon_0$  is the permittivity of the vacuum).

Equation (1) demonstrates that the dependence of  $\tilde{G}$  on the polarization components  $P_i$  corresponds to that of the standard Gibbs energy function  $G$  of a free bulk crystal. However, the coefficients of the second- and fourth-order polarization terms in these two polynomials differ from each other. Remarkably, both the mechanical film/substrate interaction and the external loading lead to a renormalization of the second-order polarization terms. As can be seen from Eqs. (2) and (3), the renormalized coefficients  $a_1^*$  and  $a_3^*$  are linear functions of the misfit strain  $S_m$  and the applied stress  $\sigma_3$ . In contrast, the introduction of this stress into the theory does not affect the renormalized fourth-order coefficients  $a_{ij}^*$ . They are defined by Eqs. (4)–(7), which coincide with the relations derived in Ref. 1 for epitaxial films with a free upper surface.

The analysis of Eqs. (2) and (3) shows that the renormalization of the second-order polarization terms in the presence of stress  $\sigma_3$  may be described by the introduction of an effective misfit strain  $S_m^\sigma$  and effective temperature  $T_\sigma$  given by the expressions

$$S_m^\sigma = S_m - (s_{11} + 2s_{12})\sigma_3, \quad (8)$$

$$T_\sigma = T - 2\varepsilon_0 C (Q_{11} + 2Q_{12})\sigma_3. \quad (9)$$

If the high-order dielectric stiffness coefficients  $a_{ij}$  and  $a_{ijk}$  are independent of temperature, Eqs. (8) and (9) provide a simple way for the evaluation of the stress effect on the polarization states of epitaxial films. In this case, the effect of external stress becomes equivalent to the changes of the misfit strain and temperature from their actual values  $S_m$  and  $T$  to the effective strain  $S_m^\sigma$  and temperature  $T_\sigma$ . Therefore, the stress-induced transformations of polarization states can be

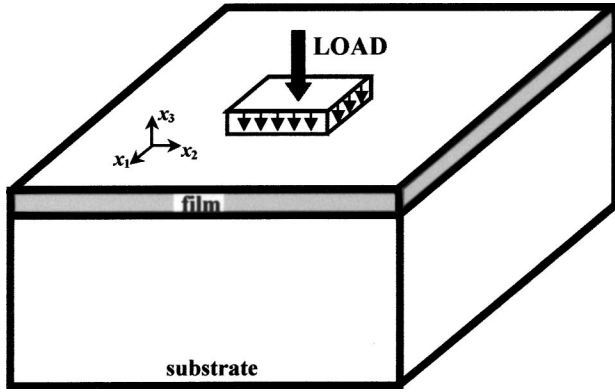


FIG. 1. Schematic of a uniform local loading of an epitaxial thin film.

predicted using the “misfit strain-temperature” phase diagrams of unloaded films and evaluating the shift in the  $(S_m, T)$  plane, which is caused by loading, from Eqs. (8) and (9). The influence of stress on single-domain states can be also determined directly from Eqs. (1)–(7). For  $\text{PbTiO}_3$  and  $\text{BaTiO}_3$  films, quantitative results may be obtained, because all their material parameters involved in the thermodynamic calculations are known to a high degree of precision.<sup>17,18</sup>

At this point it is necessary to emphasize that up to now, for clarity of presentation, we assumed the misfit strain  $S_m$  to remain constant during the film loading. However,  $S_m$  is generally a function of the applied stress since the substrate is also loaded (via the film). The influence of substrate deformations can be taken into account by adding a stress-induced change  $\Delta S_m(\sigma_3)$  to the misfit strain  $S_m = (b^* - a_0)/a_0$  of the unloaded epitaxial system. This change may be written as  $\Delta S_m = [\beta(s_{11}^{\text{sub}} + s_{12}^{\text{sub}}) + s_{12}^{\text{sub}}] \sigma_3$ , where  $s_{mn}^{\text{sub}}$  are the elastic compliances of a cubic substrate, and  $\beta$  is a geometric factor depending on the relative size of the loaded area of the substrate. If the whole substrate face is loaded,  $\beta = 0$  since the in-plane substrate deformations induced by a homogeneous stress  $\sigma_3$  are equal to  $S_1^{\text{sub}} = S_2^{\text{sub}} = s_{12}^{\text{sub}} \sigma_3$ .<sup>8</sup> In the other limiting case, where the loaded area has dimensions much smaller than those of the substrate face (but much larger than the film thickness, see Fig. 1), the deformations of the surface layer inside the loaded area are given by<sup>13</sup>  $S_1^{\text{sub}} = S_2^{\text{sub}} = (s_{11}^{\text{sub}} + 2s_{12}^{\text{sub}})(s_{11}^{\text{sub}} - s_{12}^{\text{sub}})\sigma_3/2s_{11}^{\text{sub}}$ , so that  $\beta = (s_{11}^{\text{sub}} - 2s_{12}^{\text{sub}})/2s_{11}^{\text{sub}}$ . As follows from the above relations, depending on geometry of the experimental setup, the misfit-strain change  $\Delta S_m(\sigma_3)$  may be either positive or negative at the same stress  $\sigma_3$ . Therefore, in the rest of the paper we shall consider an intermediate situation, where the stress-induced changes of the misfit strain  $S_m$  may be neglected [ $\beta \approx -s_{12}^{\text{sub}}/(s_{11}^{\text{sub}} + s_{12}^{\text{sub}})$ ]. This approach has the advantage of demonstrating *per se* the direct effect of external stress on ferroelectricity in thin films.

### III. MISFIT STRAIN-STRESS AND STRESS-TEMPERATURE DIAGRAMS OF $\text{PbTiO}_3$ AND $\text{BaTiO}_3$ EPITAXIAL FILMS

In order to describe the transformations of equilibrium thermodynamic states which may occur in epitaxial films

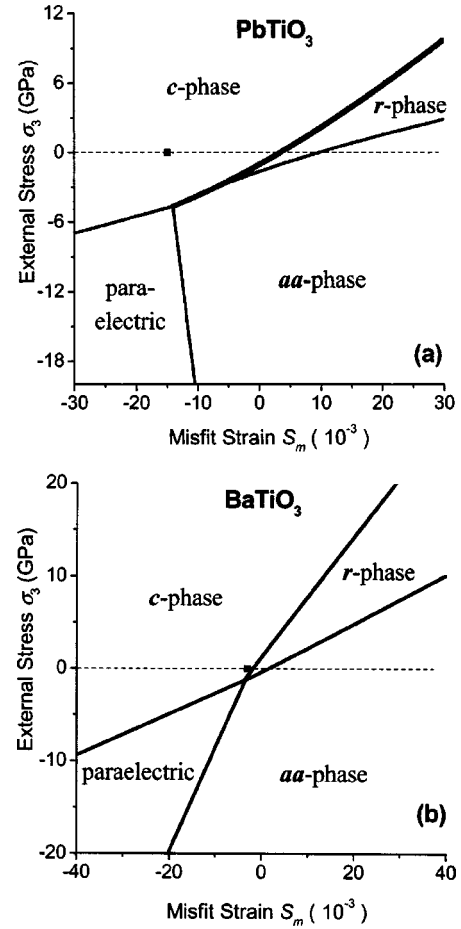


FIG. 2. Misfit strain-stress phase diagrams of single-domain  $\text{PbTiO}_3$  (a) and  $\text{BaTiO}_3$  (b) epitaxial films grown on (001)-oriented cubic substrates. The second- and first-order phase transitions are shown by thin and thick lines, respectively. The temperature is taken to be 25 °C. The square indicates the misfit strain, at which the polarization state of unloaded epitaxial film becomes equivalent to that of a bulk crystal due to the disappearance of internal stresses.

during external loading, it is useful to develop phase diagrams, where the misfit strain  $S_m$  and external stress  $\sigma_3$  are employed as two independent variables, whereas the temperature is assumed to be constant. Using Eqs. (1)–(7) with the numerical values of the involved material parameters listed in Ref. 4, we computed these “misfit strain-stress” diagrams for  $\text{PbTiO}_3$  and  $\text{BaTiO}_3$  epitaxial films under the short-circuited conditions (electric field  $\mathbf{E} = 0$  in the film). The equilibrium thermodynamic states of these films were determined by calculating all minima of the potential  $\tilde{G}$  with respect to polarization components and then selecting the energetically most favorable phase. In agreement with the results obtained in Ref. 1, the paraelectric phase ( $P_1 = P_2 = P_3 = 0$ ),  $c$  phase (tetragonal with  $P_1 = P_2 = 0, P_3 \neq 0$ ),  $aa$  phase (orthorhombic with  $P_1 = P_2 \neq 0, P_3 = 0$ ), and  $r$  phase (monoclinic with  $P_1 = P_2 \neq 0, P_3 \neq 0$ ) were found to be stable in  $\text{PbTiO}_3$  and  $\text{BaTiO}_3$  films.<sup>20</sup> The diagrams showing the stability ranges of these phases at the room temperature ( $T = 25$  °C) are presented in Fig. 2.

It can be seen that the external stress may induce various

phase transitions in ferroelectric thin films. Depending on the misfit strain  $S_m$  in the epitaxial system, the initial  $c$  phase, for instance, may transform into the  $r$  phase, the  $aa$  phase, or even into the paraelectric phase under a compressive stress  $\sigma_3 < 0$ . Though the  $c$ -phase/ $aa$ -phase transition is similar to the  $90^\circ$  polarization switching, it leads to the appearance of an *orthorhombic* lattice in the film, which does not exist in bulk  $\text{PbTiO}_3$  and  $\text{BaTiO}_3$  crystals at room temperature.<sup>17,18</sup> The stress-induced formation of the  $r$  phase is of special interest because in this *monoclinic* phase the spontaneous polarization  $\mathbf{P}_s$  has both in-plane and out-of-plane nonzero components. Compressive loading of a film containing the  $c$  phase may be a convenient technique to create unusual orthorhombic and monoclinic single-domain states in epitaxial ferroelectric films. Indeed, the nucleation of domain (twin) walls, which prevents the formation of these states in  $\text{PbTiO}_3$  and  $\text{BaTiO}_3$  films,<sup>4</sup> is expected to be suppressed at low temperatures due to kinetic reasons.

The most remarkable theoretical prediction is the ferroelectric to paraelectric phase transition induced by a compressive stress. This is an unexpected result since only the  $90^\circ$  polarization switching under mechanical stress is usually discussed for thin films in the literature.<sup>9,10</sup> During the  $c$ -phase/paraelectric-phase transformation, the film out-of-plane polarization  $P_3$  gradually decreases with increasing compressive stress  $\sigma_3$  in accordance with the relation

$$P_3^2 = -\frac{a_{33}^*}{3a_{111}} + \left( \frac{a_{33}^{*2}}{9a_{111}^2} - \frac{a_3^*}{3a_{111}} \right)^{1/2}, \quad (10)$$

where  $a_3^* = a_3^*(S_m, \sigma_3)$  and  $a_{33}^*$  are given by Eqs. (3) and (5). This monotonic decrease of  $P_3$  can produce a depolarization current similar to that observed during the microindentation of lanthanum-modified  $\text{PbTiO}_3$  films.<sup>9</sup> Such a current can be measured if the mechanical load is applied to a film sandwiched between two electrodes, as in a conventional plate-capacitor setup.

To determine the effect of loading on the film polarization states at different temperatures, we also calculated phase diagrams, where the applied stress  $\sigma_3$  and temperature  $T$  are used as two independent variables. Since the misfit strain  $S_m$  is a temperature-dependent parameter of the epitaxial system, the “stress-temperature” phase diagrams can be developed only for a given substrate. In this work, we have chosen Si as a representative substrate. As usual, it was assumed that the film is fully relaxed ( $S_m = 0$ ) at the growth temperature  $T_g$ , i.e.,  $b^*(T_g) = a_0(T_g)$ . The variation of the effective substrate lattice parameter  $b^*$  during cooling was calculated from the nonlinear temperature dependence of the lattice constant of Si, which was reported in Ref. 21. Temperature dependences of the equivalent cubic cell constants  $a_0$  of  $\text{PbTiO}_3$  and  $\text{BaTiO}_3$  crystals were determined using data<sup>18,22</sup> on their lattice constants and thermal expansion coefficients in the paraelectric phase and extrapolating  $a_0(T)$  to lower temperatures. Substituting the calculated misfit strain  $S_m(T)$  into Eqs. (1)–(3) and taking into account temperature dependences of the involved dielectric stiffnesses,<sup>17,18</sup> we developed the stress-temperature phase diagrams of  $\text{PbTiO}_3$  and  $\text{BaTiO}_3$  films grown on Si (see Fig. 3).

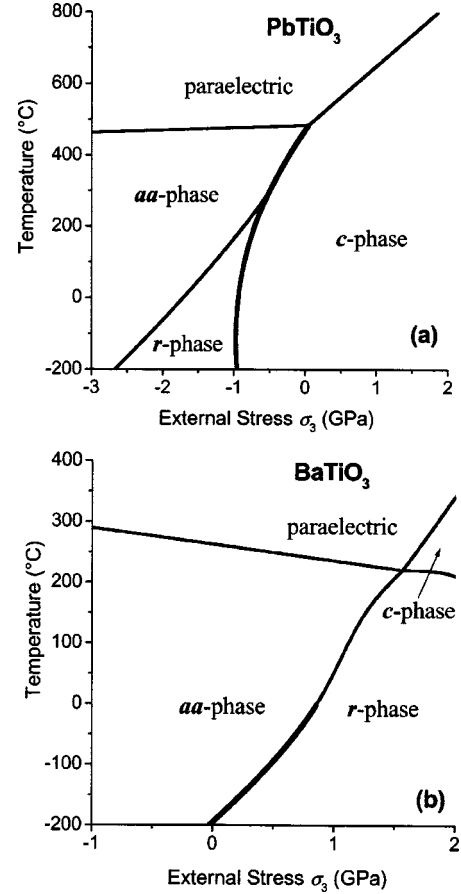


FIG. 3. Representative stress-temperature phase diagrams of single-domain  $\text{PbTiO}_3$  (a) and  $\text{BaTiO}_3$  (b) epitaxial films. The misfit strain in the film/substrate system is taken to be fully relaxed ( $S_m = 0$ ) at the growth temperature  $T_g = 800^\circ\text{C}$ . The variation of  $S_m$  during the cooling is assumed to be totally controlled by the difference in thermal expansion coefficients of the film and substrate. The dependence  $S_m(T)$  corresponds to films deposited on silicon.

The calculations showed that the mechanical loading does not change the order of the paraelectric to ferroelectric phase transition, which remains of second order as in unloaded single-domain films.<sup>1</sup> The ferroelectric transition temperature *decreases* with increasing magnitude of compressive stress  $\sigma_3 < 0$  and rises with increasing tensile stress  $\sigma_3 > 0$  in the case of  $\text{PbTiO}_3$  films. In contrast, this temperature *increases* with increasing compressive stress and varies nonmonotonically with tensile stress in  $\text{BaTiO}_3$  films. Accordingly, by creating sufficient tensile stress in the  $\text{BaTiO}_3$  film at a high temperature ( $\sim 250^\circ\text{C}$  for the discussed substrate), it is possible to convert the ferroelectric  $aa$  phase into the paraelectric one. At low temperatures, the application of a tensile stress may induce the  $aa$ -phase/ $r$ -phase transformation [see Fig. 3(b)].

Using the developed nonlinear thermodynamic theory, we also analyzed the possibility of ferroelastolectric switching<sup>10</sup> in  $\text{BaTiO}_3$  and  $\text{PbTiO}_3$  films subjected to both compressive stress  $\sigma_3$  and electric field  $\mathbf{E}$ . In accordance with the model employed in Ref. 10, it was assumed that the polarization  $\mathbf{P}$  in a film remains oriented along the substrate



normal ( $P_1=P_2=0$ ,  $P_3\neq 0$ ) at all values of the applied stress  $\sigma_3$ . To make this assumption realistic, the misfit strain  $S_m$  in the film/substrate system was set negative and large enough to avoid transformations of the initial  $c$  phase into the  $aa$  and  $r$  phases during the loading at room temperature (see Fig. 2). The applied electric field  $\mathbf{E}$  was supposed to be homogeneous and orthogonal to the film surfaces ( $E_1=E_2=0, E_3\neq 0$ ), as in a conventional plate-capacitor setup. To take into account the influence of this field on the film polarization  $P_3$ , the latter was calculated from the equation  $\partial\tilde{G}/\partial P_3=E_3$ . Two possible solutions for the equilibrium polarization  $P_3(\mathbf{E})$ , i.e., parallel and antiparallel to the applied field  $\mathbf{E}$ , were analyzed, and the corresponding extreme values of the modified thermodynamic potential  $\tilde{G}$  were compared. During the calculations, the applied compressive stress was increased from zero up to several GPa, whereas the electric field was varied in a wide range between zero and  $10^8$  V/m. It was found that the antiparallel orientation of polarization with respect to the electric field  $\mathbf{E}$  never appears to be energetically more favorable than the parallel orientation. Moreover, at compressive stresses of several GPa, which were predicted in Ref. 10 to be sufficient for ferroelastoelectric switching, the spontaneous polarization  $\mathbf{P}_s(\mathbf{E}=0)$  vanishes in epitaxial films (see Fig. 2). The ferroelectric  $c$  phase transforms here into the paraelectric one, where the polarization cannot be oriented against the field  $\mathbf{E}$ . Thus, the nonlinear thermodynamic theory does not support the prediction of the stress-induced  $180^\circ$  switching of polarization into the direction antiparallel to the applied electric field, which was made in Ref. 10 using the linear approximation.

#### IV. DIELECTRIC AND PIEZOELECTRIC PROPERTIES OF UNIFORMLY LOADED $\text{PbTiO}_3$ AND $\text{BaTiO}_3$ FILMS

Since the stress-induced phase transitions may be accompanied by dielectric and piezoelectric anomalies, we discuss in this section the small-signal dielectric and piezoelectric responses of loaded ferroelectric films. The film dielectric constants  $\varepsilon_{ij}$  can be calculated from the reciprocal dielectric susceptibilities  $\chi_{ij}=\partial^2\tilde{G}/\partial P_i\partial P_j$ , which are found by direct differentiation of the modified thermodynamic potential  $\tilde{G}$ . In general, all components of the matrix  $\chi_{ij}$  must be determined to compute the dielectric constant  $\varepsilon_{kl}=\varepsilon_0+\eta_{kl}$ , because the matrix of dielectric susceptibilities  $\eta_{ij}$  is the inverse of  $\chi_{ij}$ , and the latter is diagonal only in the  $c$  phase. By substituting the equilibrium values  $P_i(\mathbf{E}=0)$  of the polarization components into the expressions derived for  $\chi_{ij}$  via Eq. (1), it is possible to calculate the small-signal dielectric responses  $\varepsilon_{ij}$  of epitaxial ferroelectric films as functions of the misfit strain, temperature, and external stress. For the out-of-plane permittivity  $\varepsilon_{33}$  of the  $c$  phase, e.g., the calculation yields

$$\varepsilon_{33}=\varepsilon_0+(2a_3^*+12a_{33}^*P_3^2+30a_{111}P_3^4)^{-1}, \quad (11)$$

where  $P_3$  is given by Eq. (10).

Performing necessary numerical computations, we determined the effect of external loading on the dielectric constants of  $\text{PbTiO}_3$  and  $\text{BaTiO}_3$  films. Figures 4 and 5 show

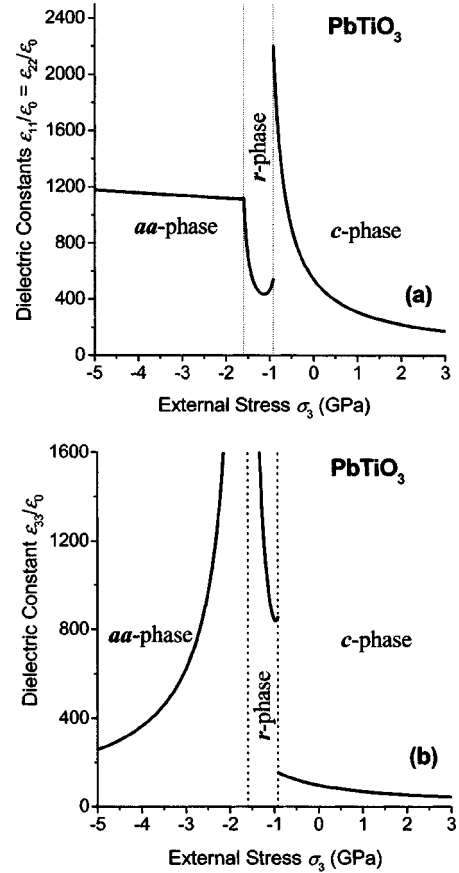


FIG. 4. Dependences of the dielectric constants  $\varepsilon_{11}=\varepsilon_{22}$  (a) and  $\varepsilon_{33}$  (b) of single-domain  $\text{PbTiO}_3$  films on the external stress  $\sigma_3$  at  $T=25^\circ\text{C}$ . The misfit strain is taken to be  $S_m=4.9\times 10^{-4}$ , which corresponds to the silicon substrate and the deposition at  $T_g=800^\circ\text{C}$ .

variations of the diagonal components  $\varepsilon_{ii}$  ( $i=1,2,3$ ) of the dielectric tensor with the applied stress  $\sigma_3$  at room temperature. (The misfit strain  $S_m$  in the film/substrate system was taken to be  $4.9\times 10^{-4}$  for  $\text{PbTiO}_3$  and  $5.2\times 10^{-3}$  for  $\text{BaTiO}_3$ , which corresponds to the silicon substrate and  $T=25^\circ\text{C}$ .) In the case of a  $\text{PbTiO}_3$  film, the application of a compressive stress leads to a strong increase of the in-plane dielectric responses  $\varepsilon_{11}=\varepsilon_{22}$  of the  $c$  phase. They reach values in excess of 2000 at stresses close to  $\sigma_3\cong -0.92$  GPa, at which the first-order  $c$ -phase/ $r$ -phase transition takes place. The out-of-plane permittivity  $\varepsilon_{33}$  experiences a jump at this critical stress and then continues to increase at larger stresses, diverging at the second-order  $r$ -phase/ $aa$ -phase transition. In contrast, the compressive loading of a  $\text{BaTiO}_3$  film, which is initially in the in-plane polarization state (the  $aa$  phase), leads to the reduction of all the dielectric constants  $\varepsilon_{ii}$ . By creating a strong tensile stress in the film, however, it would be possible to increase the permittivities  $\varepsilon_{ii}$  significantly (see Fig. 5). This effect is due to the stress-induced second-order phase transitions in  $\text{BaTiO}_3$  films [Fig. 2(b)]. Theoretically, the permittivities  $\varepsilon_{33}$  and  $\varepsilon_{11}=\varepsilon_{22}$  should diverge at the  $aa$ -phase/ $r$ -phase and  $r$ -phase/ $c$ -phase transitions, respectively. However, the increase of the film permittivity, which could be observed experimentally, is limited due to extrinsic factors.

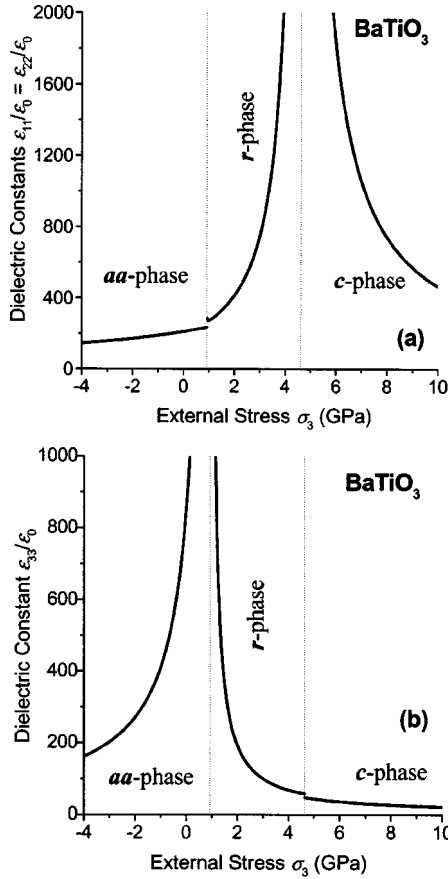


FIG. 5. Dependences of the dielectric constants  $\epsilon_{11} = \epsilon_{22}$  (a) and  $\epsilon_{33}$  (b) of single-domain BaTiO<sub>3</sub> films on the external stress  $\sigma_3$  at  $T = 25^\circ\text{C}$ . The misfit strain is taken to be  $S_m = 5.2 \times 10^{-3}$ , which corresponds to the silicon substrate and the deposition at  $T_g = 800^\circ\text{C}$ .

Let us now proceed to the theoretical description of the piezoelectric properties of loaded ferroelectric thin films. For simplicity, we shall restrict our analysis to the converse piezoelectric effect displayed by a thin film in a plate-capacitor setup. Since the epitaxial film is rigidly connected with a thick substrate, the application of an electric field  $E_3$  orthogonal to the film surfaces may result only in a change of the film thickness and a tilt of the ferroelectric overlayer relative to the substrate normal. These effects are determined by the piezoelectric coefficients  $d_{33}$ ,  $d_{34}$ , and  $d_{35}$ . In general, the constants  $d_{in}$  are calculated as  $d_{in} = \partial S_n / \partial E_i = b_{kn} \eta_{ki}$ , where  $b_{kn} = \partial S_n / \partial P_k$ . The strains  $S_n = -\partial G / \partial \sigma_n$  may be found as functions of the polarization components  $P_i$  and stresses  $\sigma_n$  by differentiating the standard Gibbs free energy  $G$ . Taking into account the mechanical boundary conditions, we find the variable lattice strains in a loaded epitaxial film as

$$S_3 = \frac{2s_{12}}{s_{11} + s_{12}} (S_m - s_2 \sigma_3) + s_{11} \sigma_3 + \left[ Q_{12} - \frac{s_{12}(Q_{11} + Q_{12})}{s_{11} + s_{12}} \right] \times (P_1^2 + P_2^2) + \left( Q_{11} - \frac{2s_{12}Q_{12}}{s_{11} + s_{12}} \right) P_3^2,$$

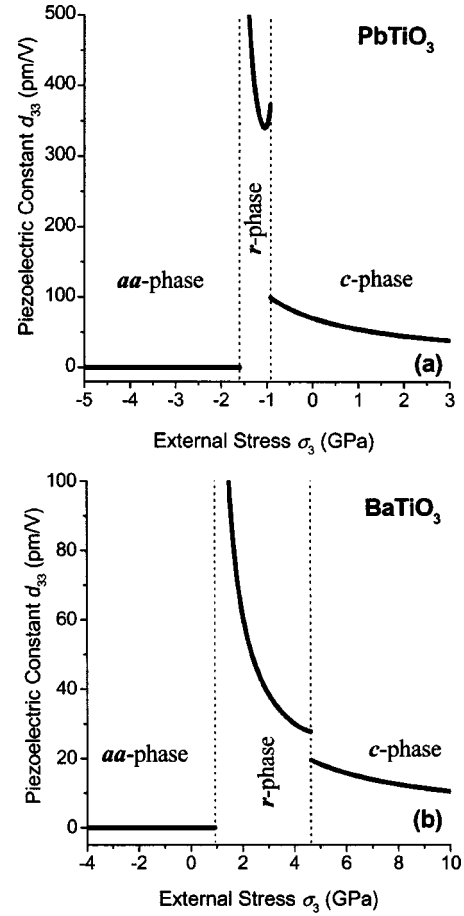


FIG. 6. Dependence of the longitudinal piezoelectric coefficient  $d_{33}$  on the external stress  $\sigma_3$  calculated for single-domain PbTiO<sub>3</sub> (a) and BaTiO<sub>3</sub> (b) films at  $T = 25^\circ\text{C}$ . The misfit strain  $S_m$  is taken to be  $4.9 \times 10^{-4}$  (a) and  $5.2 \times 10^{-3}$  (b), which correspond to the Si substrate and  $T_g = 800^\circ\text{C}$ .

$$S_4 = Q_{44} P_2 P_3, \quad S_5 = Q_{44} P_1 P_3. \quad (12)$$

The differentiation of these relations makes it possible to calculate the relevant constants  $b_{kn}$  using the known equilibrium values  $P_i(\mathbf{E} = 0)$  of the polarization components. Since the small-signal dielectric susceptibilities  $\eta_{ki}$  of loaded films are already determined, the piezoelectric constants  $d_{33}$ ,  $d_{34}$ , and  $d_{35}$  can be finally calculated as functions of the misfit strain  $S_m$ , temperature  $T$ , and external stress  $\sigma_3$ .

Figure 6 shows the dependence of the longitudinal piezoelectric coefficient  $d_{33}$  of PbTiO<sub>3</sub> and BaTiO<sub>3</sub> films on the applied stress at room temperature. It can be seen that the piezoelectric response of the  $c$  phase, which represents the stable single-domain state in PbTiO<sub>3</sub> films at the chosen misfit strain  $S_m = 4.9 \times 10^{-4}$ , increases under compressive loading. The piezoelectric coefficient  $d_{33}$  experiences a jump at the critical stress  $\sigma_3 \cong -0.92$  GPa, at which the  $c$  phase transforms into the  $r$  phase, and then becomes anomalously high at the  $r$ -phase/ $aa$ -phase transition. On the other hand, the BaTiO<sub>3</sub> film is initially in the  $aa$  phase ( $S_m = 5.2 \times 10^{-3}$ ), so that  $d_{33}$  remains zero irrespective of the compressive stress. In contrast, a tensile stress applied to the BaTiO<sub>3</sub> film might drastically increase the piezoelectric con-

stant  $d_{33}$  since at the critical stress  $\sigma_3 \cong 0.925$  GPa the  $aa$  phase transforms into the  $r$  phase, which displays a strong piezoelectric response near the critical stress.

## V. CONCLUSIONS

The nonlinear thermodynamic theory predicts that the external loading may have a strong impact on the polarization state and physical properties of ferroelectric thin films. First and foremost, the compressive loading of thin films grown on “compressive” substrates, which provide large negative misfit strains in the epitaxial system, may transform the ferroelectric phase into the paraelectric one even at temperatures well below the Curie temperature of a bulk material (e.g., at room temperature). Second, the external stress may induce the rotation of the spontaneous polarization  $\mathbf{P}_s$  relative to the film plane, resulting in the transition from the out-of-plane polarization state to the in-plane one. Third, the dielectric and piezoelectric constants of ferroelectric films may dramatically increase under the influence of applied stress. Therefore, the external loading provides an effective technique for improving the performances of ferroelectric thin films, which are necessary for their applications in microelectronic devices and microelectromechanical systems (MEMS). In addition, the stability of spontaneous polarization under the stresses developed during the device operation represents an important factor in determining the limits of applicability of MEMS, which employ the piezoelectric properties of ferroelectric thin films.

We believe that the phase transformations predicted in this paper can occur during the *nanoscale loading* of ferroelectric thin films via the SFM tip. Indeed, the highly stressed region  $V_\sigma$  under the tip has very small dimensions of the order of the contact radius ( $\sim 10$  nm). In this case, the stress-induced twinning of the strained subsurface region becomes energetically unfavorable due to the size effect (in  $\text{PbTiO}_3$ , e.g., the threshold size is about 50 nm; see Ref. 23). Therefore, in the absence of preexisting ferroelastic domain walls in the probed volume, only phase transitions between different single-domain states are expected to take place un-

der the tip. It should be emphasized that the phase evolution may involve a continuous rotation of the polarization vector  $\mathbf{P}_s$  and a gradual change of its magnitude. This nanoscale behavior is in contrast to the formation and motion of multiple  $90^\circ$  domain walls, which represents the most probable relaxation mechanism in the films subjected to microindentation.<sup>9</sup>

The stresses  $\sigma_n(\mathbf{r})$  induced in a thin film by the SFM tip can be estimated using the Hertzian elastic approximation for the spherical indentation.<sup>14</sup> For  $\text{BaTiO}_3$  and  $\text{PbTiO}_3$  films loaded via silicon tips with a radius of about 10 nm, the calculation gives the mean stress  $\langle \sigma_3 \rangle \sim -10$  GPa in the probed volume  $V_\sigma \sim 10^3$  nm<sup>3</sup> under the tip at the applied forces  $f \sim 10^{-6}$  N used experimentally.<sup>10,12</sup> As can be seen from Fig. 2, this compressive stress is high enough to transform the out-of-plane polarization state ( $c$  phase) into the paraelectric phase or into the in-plane polarization state ( $aa$  phase). Such a transformation will be accompanied by a strong decrease of the nanoscale piezoelectric response  $d_{33}$  of a ferroelectric film measured with the aid of the SFM.<sup>24</sup> Since the transformed nanoscale region is surrounded by a different (initial) phase, the decrease of  $d_{33}$  at high applied forces  $f$  must be reversible, as observed experimentally in Ref. 12.

Finally, it should be noted that the spherical indentation creates not only the normal stress  $\sigma_3$  in the film, but also the in-plane stresses  $\sigma_1$  and  $\sigma_2$ .<sup>14</sup> Since just under the tip these stresses are compressive and close to  $\sigma_3$ , their influence on the film polarization state is similar to the introduction of an additional negative misfit strain  $\Delta S_m < 0$  into the epitaxial system. Therefore, the stress state just under the SFM tip promotes the ferroelectric to paraelectric phase transition.

## ACKNOWLEDGMENT

The research described in this publication was made possible in part by a grant from the Foundation for Science and Technology of Portugal (Project No. POCTI/35502/CTM/2000).

\*Corresponding author.

Electronic address: pertsev@domain.ioffe.rssi.ru

<sup>1</sup>N. A. Pertsev, A. G. Zembilgotov, and A. K. Tagantsev, *Phys. Rev. Lett.* **80**, 1988 (1998); *Ferroelectrics* **223**, 79 (1999).

<sup>2</sup>N. A. Pertsev, A. K. Tagantsev, and N. Setter, *Phys. Rev. B* **61**, R825 (2000); **65**, 219901 (2002).

<sup>3</sup>N. A. Pertsev and V. G. Koukhar, *Phys. Rev. Lett.* **84**, 3722 (2000).

<sup>4</sup>V. G. Koukhar, N. A. Pertsev, and R. Waser, *Phys. Rev. B* **64**, 214103 (2001).

<sup>5</sup>Y. L. Li, S. Y. Hu, Z. K. Liu, and L. Q. Chen, *Appl. Phys. Lett.* **78**, 3878 (2001).

<sup>6</sup>A. K. Tagantsev, N. A. Pertsev, P. Muralt, and N. Setter, *Phys. Rev. B* **65**, 012104 (2002).

<sup>7</sup>Z.-G. Ban and S. P. Alpay, *J. Appl. Phys.* **91**, 9288 (2002).

<sup>8</sup>K. Lefki and G. J. M. Dormans, *J. Appl. Phys.* **76**, 1764 (1994).

<sup>9</sup>M. Alguero, A. J. Bushby, M. J. Reece, R. Poyato, J. Ricote, M.

L. Calzada, and L. Pardo, *Appl. Phys. Lett.* **79**, 3830 (2001).

<sup>10</sup>M. Abplanalp, J. Fousek, and P. Günter, *Phys. Rev. Lett.* **86**, 5799 (2001).

<sup>11</sup>A. Gruverman, O. Auciello, and H. Tokumoto, *Annu. Rev. Mater. Sci.* **28**, 101 (1998).

<sup>12</sup>G. Zavala, J. H. Fendler, and S. Troiler-McKinstry, *J. Appl. Phys.* **81**, 7480 (1997).

<sup>13</sup>K. L. Johnson, *Contact Mechanics* (Cambridge University Press, Cambridge, 1985).

<sup>14</sup>B. R. Lawn, *J. Am. Ceram. Soc.* **81**, 1977 (1998).

<sup>15</sup>A. E. Giannakopoulos and S. Suresh, *Acta Mater.* **47**, 2153 (1999).

<sup>16</sup>S. Sridhar, A. E. Giannakopoulos, S. Suresh, and U. Ramamurty, *J. Appl. Phys.* **85**, 380 (1999).

<sup>17</sup>A. J. Bell and L. E. Cross, *Ferroelectrics* **59**, 197 (1984).

<sup>18</sup>M. J. Haun, E. Furman, S. J. Jang, H. A. McKinstry, and L. E. Cross, *J. Appl. Phys.* **62**, 3331 (1987).

<sup>19</sup>J. S. Speck and W. Pompe, J. Appl. Phys. **76**, 466 (1994).

<sup>20</sup>In BaTiO<sub>3</sub>, the monoclinic *ca* phase ( $P_1 \neq 0$ ,  $P_2 = 0$ ,  $P_3 \neq 0$ ) is also stable at low temperatures in a narrow misfit-strain range, but this phase does not appear on the diagrams reported in this paper.

<sup>21</sup>*Physics of Group IV Elements and III-V Compounds*, edited by O. Madelung, Landolt-Börnstein, New Series, Group III, Vol. 17, Pt(a) (Springer-Verlag, Berlin, 1982), p. 61.

<sup>22</sup>Y. S. Touloukian, R. K. Kirby, R. E. Taylor, and T. Y. R. Lee,

*Thermal Expansion, Nonmetallic Solids*, Thermophysical Properties of Matter Vol. 13 (Plenum, New York, 1997).

<sup>23</sup>N. A. Pertsev and E. K. H. Salje, Phys. Rev. B **61**, 902 (2000).

<sup>24</sup>Owing to the strong inhomogeneity of the stress field under the scanning force microscopy tip, the variation of the nanoscale response  $d_{33}$  at small applied forces  $f \ll 10^{-6}$  N may differ significantly from the dependence  $d_{33}(\langle \sigma_3 \rangle)$  calculated in our approximation.